How Ionic Are Room-Temperature Ionic Liquids? An Indicator of the Physicochemical Properties

Hiroyuki Tokuda,[†] Seiji Tsuzuki,[‡] Md. Abu Bin Hasan Susan,[†,||] Kikuko Hayamizu,[§] and Masayoshi Watanabe*,[†]

Department of Chemistry and Biotechnology, Yokohama National University, and CREST-JST, 79-5 Tokiwadai, Hodogaya-ku, Yokohama 240-8501, Japan, AIST Tsukuba Centre 2, National Institute of Advanced Industrial Science and Technology, Tsukuba 305-8568, Japan, and AIST Tsukuba Centre 5, National Institute of Advanced Industrial Science and Technology, Tsukuba 305-8565, Japan

Room-temperature ionic liquids (RTILs) are liquids consisting entirely of ions, and their important properties, e.g., negligible vapor pressure, are considered to result from the ionic nature. However, we do not know how ionic the RTILs are. The ionic nature of the RTILs is defined in this study as the molar conductivity ratio ($\Lambda_{imp}/\Lambda_{NMR}$), calculated from the molar conductivity measured by the electrochemical impedance method (Λ_{imp}) and that estimated by use of pulse-field-gradient spin–echo NMR ionic self-diffusion coefficients and the Nernst–Einstein relation (Λ_{NMR}). This ratio is compared with solvatochromic polarity scales: anionic donor ability (Lewis basicity), $E_T(30)$, hydrogen bond donor acidity (α), and dipolarity/polarizability (π^*), as well as NMR chemical shifts. The $\Lambda_{imp}/\Lambda_{NMR}$ well illustrates the degree of cation–anion aggregation in the RTILs at equilibrium, which can be explained by the effects of anionic donor and cationic acceptor abilities for the RTILs having different anionic and cationic backbone structures with fixed counterparts, and by the inductive and dispersive forces for the various alkyl chain lengths in the cations. As a measure of the electrostatic interaction of the RTILs, the effective ionic concentration (C_{eff}), which is a dominant parameter for the electrostatic forces of the RTILs, was introduced as the product of $\Lambda_{imp}/\Lambda_{NMR}$ and the molar concentration and was compared with some physical properties, such as reported normal boiling points and distillation rates, glass transition temperature, and viscosity. A decrease in C_{eff} of the RTILs is well correlated with the normal boiling point and distillation rate, whereas the liquid-state dynamics is controlled by a subtle balance between the electrostatic and other intermolecular forces.

Introduction

Great interest has been taken in room-temperature ionic liquids (RTILs), due to their potential as new chemical, catalytic, and electrochemical reaction media with negligible vapor pressure.[1,2] Since the syntheses are highly flexible and are capable of tailoring the size, shape, and functionality of the component cations and anions, their numerous combinations offer great opportunities for tuning the physicochemical properties. Thus the design of RTILs has become one of the most fascinating domains of current chemical research. For the design, however, it is necessary to establish a key parameter that would make it possible to characterize their physicochemical properties. For molecular solvents, to understand the solvent effects on chemical reactions and physicochemical phenomena, many empirical solvent polarity scales have been proposed in past decades, such as the *Z* scale of Kosower,[3] the *Y* scale of

Winstein,[4] the $E_T(30)$ scale of Dimroth and Reichardt,[5] the Py (or pyrene) scale of Dong and Winnik,[6] the Kamlet and Taft parameters (α, β, and π^*),[7] and Gutmann's donor (DN) and acceptor numbers (AN).[8] In particular, it has been well recognized that the donor–acceptor approach, based on electron-donor (Lewis basic or nucleophilic) and electron-acceptor (Lewis acidic or electrophilic) abilities of a solvent and a solute, can simply describe solvent effects such as molecular aggregation, ionic solvation, and ionization equilibria in organic and coordination chemistries.[8]

The subject of a number of studies has been to experimentally[9–23] and theoretically[24–29] correlate the ionic structures of the RTILs with the physicochemical properties, including preparation of novel ionic liquids by combining new cations and anions, studies of their properties, and theoretical calculations and simulations. Most of the RTILs reported to date can be classified as combinations of weakly Lewis acidic cations and weakly Lewis basic anions, which leads to ionic dissociation without strong coordination of solvent molecules around each ion. This point clearly contrasts the situation with typical ionic crystals. In this sense, RTILs can be recognized as "self-dissociable liquid salts" at room temperature. The ionic nature ("ionicity" or "how ionic?") in the liquid state contributes to the realization of negligibly small vapor pressure, which is the

* To whom correspondence should be addressed. Fax: +81-45-339-3955. E-mail: mwatanab@ynu.ac.jp.
† Yokohama National University and CREST–JST.
‡ AIST Tsukuba Centre 2, National Institute of Advanced Industrial Science and Technology.
§ AIST Tsukuba Centre 5, National Institute of Advanced Industrial Science and Technology.
|| Permanent address: Department of Chemistry, University of Dhaka, Dhaka 1000, Bangladesh.

19594 *J. Phys. Chem. B, Vol. 110, No. 39, 2006*

Tokuda et al.

most distinguished property compared to conventional molecular solvents. Quantitative description of the ionicity can, therefore, be a useful indicator with which the RTILs are characterized.

In a series of our studies, we have reported quantitative information on the formation of ionic aggregates in RTILs based on the ratios of molar conductivity values ($\Lambda_{imp}/\Lambda_{NMR}$), where Λ_{imp} is the molar conductivity obtained by electrochemical impedance measurements and Λ_{NMR} is that calculated from the pulse-field-gradient spin−echo NMR (PGSE-NMR) ionic self-diffusion coefficients and the Nernst−Einstein equation.[30,31] The Λ_{NMR} value assumes that all of the diffusing species detected by the PGSE-NMR measurements contribute to the molar conductivity. On the other hand, the Λ_{imp} value is based on the migration of the charged species under an electric field. The $\Lambda_{imp}/\Lambda_{NMR}$ ratio, therefore, indicates the percentage of ions (charged species) contributing to the ionic conduction in the diffusing species on the time scale of the measurements. The $\Lambda_{imp}/\Lambda_{NMR}$ ratio may be correlated with the ionicity of the RTILs and is shown in this study to be a useful parameter with which to characterize the significant properties of the RTILs. The conductivity ratios have been developed to elucidate discrepancies between the structural relaxation time and the conduction relaxation time in ion-conductive glasses,[32] and more recent studies have provided insight into the ion transport behavior of aprotic electrolyte solutions.[33]

Here, we present experimental correlations of $\Lambda_{imp}/\Lambda_{NMR}$ with the solvatochromic polarity scales of the RTILs.[34−46] It should be noted here that the reported polarity scales of hydrogen bond donor (HBD) acidity, α, and $E_T(30)$ depend mainly on the cation, whereas those of hydrogen bond acceptor (HBA) basicity, β, and the donor ability depend on the anion.[35−38] In contrast, $\Lambda_{imp}/\Lambda_{NMR}$ is a unique parameter for each RTIL, with a small temperature dependency.[30,31] A comparison of the polarity scales with the $\Lambda_{imp}/\Lambda_{NMR}$ ratio would, therefore, help us understand how the ionic structure affects the ionic nature of the RTILs through their interionic and intermolecular interactions. Furthermore, the effective ionic concentrations may be estimated as products of the molar concentration and the $\Lambda_{imp}/\Lambda_{NMR}$ ratios. The cubic root of the reciprocal of the effective ionic concentration can represent the effective interionic distance. Since the main interactions in the RTILs are Coulombic, the ionic structural effects on the physical properties are also discussed as a function of the effective ionic concentration in order to understand how the Coulombic forces dominate the properties.

Results

$\Lambda_{imp}/\Lambda_{NMR}$ **and** C_{eff} **of RTILs.** Table 1 summarizes the physicochemical properties of the RTILs at 30 °C, including the glass transition temperature (T_g), melting temperature (T_m), density (ρ), molar concentration (M, based on ρ and the molecular weight), viscosity (η), self-diffusion coefficients of cation (D_+) and anion (D_-), ionic conductivity (σ), and molar conductivity (Λ_{imp}, obtained from σ and M).[31] These values are presented for the whole measured temperature range in the Supporting Information, parts 1−4. The molar conductivity (Λ_{NMR}) can also be calculated from the ionic self-diffusion coefficients, using the Nernst−Einstein equation:

$$\Lambda_{NMR} = N_A e^2 (D_+ + D_-)/kT \qquad (1)$$

where N_A is the Avogadro number, e is the electric charge on each ionic carrier, k is the Boltzmann constant, and T is the absolute temperature. The molar conductivity ratio, $\Lambda_{imp}/\Lambda_{NMR}$,

is also listed in Table 1. It is clear that the $\Lambda_{imp}/\Lambda_{NMR}$ values for all of the RTILs in this study are less than unity, indicating that not all of the diffusive species in the RTILs contribute to the ionic conduction; i.e., ionic aggregates and/or clusters are formed. It should be noted here that the NMR measurements cannot distinguish associated ionic species from free ions within the intrinsic NMR time scale (10^{-9}−10^{-10} s). This implies that the time scales for the association/dissociation processes of the ionic species, if any, are much shorter than those of the conductivity measurements. In the latter time scale, an individual ion migrates under an electric field for a certain characteristic time when it exists as a charged species, but it may associate to form a noncharged aggregate for another characteristic time. When the ion exists as a noncharged species, it does not contribute to the conduction. Another reason for the $\Lambda_{imp}/\Lambda_{NMR}$ values being less than unity is that strong interactions between the ions decrease the ionic activity to some extent.

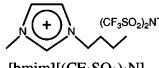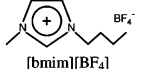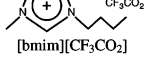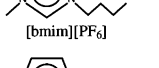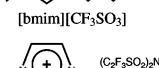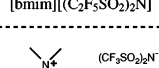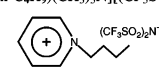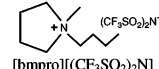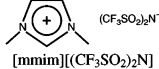For the [bmim]-based RTILs with different anionic structures (Table 1, entries 1−6), $\Lambda_{imp}/\Lambda_{NMR}$ ranges from 0.52 to 0.68 and follows the order [PF$_6$] > [BF$_4$] ≈ [(C$_2$F$_5$SO$_2$)$_2$N] > [(CF$_3$-SO$_2$)$_2$N] > [CF$_3$SO$_3$] > [CF$_3$CO$_2$]. For the [(CF$_3$SO$_2$)$_2$N]-based RTILs with the same substituent butyl group in different cationic backbone structures (entries 1 and 7−9), it ranges from 0.61 to 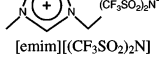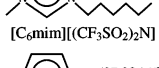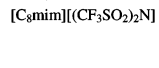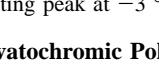0.70, and the order is [bmpro] > [(*n*-C$_4$H$_9$)(CH$_3$)$_3$N] > [bpy] > [bmim]. The $\Lambda_{imp}/\Lambda_{NMR}$ values of the [Rmim][(CF$_3$SO$_2$)$_2$N] RTILs (entries 1 and 10−13) decrease from 0.76 to 0.54 with increasing number of carbon atoms in the alkyl chain in the imidazolium moiety.

The effective ionic concentration, C_{eff}, the product of $\Lambda_{imp}/\Lambda_{NMR}$ and molar concentration, is also listed in Table 1. For the [bmim]-based RTILs with different anionic structures (entries 1−6), C_{eff} ranges from 1.8×10^{-3} to 3.4×10^{-3} mol cm^{-3} and follows the order [BF$_4$] > [PF$_6$] > [CF$_3$SO$_3$] > [CF$_3$-CO$_2$] > [(CF$_3$SO$_2$)$_2$N] > [(C$_2$F$_5$SO$_2$)$_2$N]. The C_{eff} values of the [Rmim][(CF$_3$SO$_2$)$_2$N] RTILs (entries 1 and 10−13) decreases from 3.1×10^{-3} to 1.5×10^{-3} mol cm^{-3} with increasing alkyl chain length. On the other hand, the [(CF$_3$SO$_2$)$_2$N]-based RTILs with different cationic backbone structures (entries 1 and 7−9) have almost the same C_{eff} values [$(2.1−2.3) \times 10^{-3}$ mol cm^{-3}].

Solvatochromic Polarity Scales of RTILs. The solvatochromic polarity scales of the RTILs were investigated with the use of three different kinds of dyes, [Cu(acac)(tmen)]BPh$_4$ (acac = acetylacetone, tmen = *N,N,N′,N′*-tetramethylethylenediamine), 2,6-diphenyl-4-(2,4, 6-triphenyl-*N*-pyridino)phenolate (Reichardt's betaine dye), and *N,N*-diethyl-4-nitroaniline (DENA). The estimated polarity scales of the RTILs are listed in Table 2, and the values of this study are in good agreement with those from the literature.[35−38]

It is well-known that [Cu(acac)(tmen)][BPh$_4$] gives a good correlation between the DN of a solvent and the absorption maximum wavelength (λ_{Cu}), corresponding to the lowest energy d−d absorption bands, derived from changes in the splitting of the d-orbitals of the Cu^{2+} ion due to five- and six-coordination.[45] This method has been expanded for the estimation of anionic DNs in several organic solutions.[46] As can be seen in Table 2, no specific shift of the λ_{Cu} could be obtained in the case of the [(CF$_3$SO$_2$)$_2$N]-based RTILs with different cationic structures (entries 1 and 7−13). On the other hand, the λ_{Cu} of the [bmim]-based RTILs shifted drastically with changes in the anionic structures (entries 1−6), which corresponds to a wide change in the DN values in molecular solvents.[45b] It can be seen from Table 2 that the anionic donor ability follows the order [CF$_3$-CO$_2$] > [CF$_3$SO$_3$] > [(CF$_3$SO$_2$)$_2$N] > [(C$_2$F$_5$SO$_2$)$_2$N] ≈ [BF$_4$] > [PF$_6$].

Physicochemical Properties of RTILs

J. Phys. Chem. B, Vol. 110, No. 39, 2006 **19595**

TABLE 1: Physical Properties of Room-Temperature Ionic Liquids at 30 °C

Entry	RTILs	T_g /°C	T_m /°C	ρ /gcm⁻³	M/10⁻³ molcm⁻³	η /mPas	D_+ /10⁻⁷cm²s⁻¹	D_-	σ/10⁻³ Scm⁻¹	Λ_{imp} /Scm²mol⁻¹	$\Lambda_{imp}/\Lambda_{NMR}$ /-	C_{eff}/10⁻³ molcm⁻³
1	[bmim][(CF₃SO₂)₂N]	-87	-3	1.43	3.42	40	3.4	2.6	4.6	1.4	0.61	2.1
2	[bmim][BF₄]	-83		1.20	5.30	75	1.8	1.8	4.5	0.85	0.64	3.4
3	[bmim][CF₃CO₂]	-78		1.21	4.81	58	2.2	1.9	3.8	0.80	0.52	2.5
4	[bmim][PF₆]	-77	10	1.37	4.80	182	0.89	0.71	1.9	0.40	0.68	3.3
5	[bmim][CF₃SO₃]	-82ᵃ	17	1.29	4.49	64	2.2	1.6	3.6	0.80	0.57	2.6
6	[bmim][(C₂F₅SO₂)₂N]	-84		1.51	2.91	87	1.6	1.1	1.9	0.64	0.63	1.8
7	[(n-C₄H₉)(CH₃)₃N][(CF₃SO₂)₂N]	-74	19	1.39	3.50	77	1.7	1.4	2.6	0.74	0.65	2.3
8	[bpy][(CF₃SO₂)₂N]	-76ᵃ	26	1.44	3.47	49	2.8	2.2	4.0	1.2	0.63	2.2
9	[bmpro][(CF₃SO₂)₂N]	-83	-15ᵇ	1.39	3.29	60	2.2	1.8	3.4	1.0	0.70	2.3
10	[mmim][(CF₃SO₂)₂N]		26	1.57	4.15	31	5.8	3.3	11	2.5	0.76	3.1
11	[emim][(CF₃SO₂)₂N]	-87ᵃ	-18	1.51	3.87	27	6.2	3.7	11	2.7	0.75	2.9
12	[C₆mim][(CF₃SO₂)₂N]	-81	-6	1.37	3.05	56	2.2	1.9	2.7	0.87	0.57	1.8
13	[C₈mim][(CF₃SO₂)₂N]	-80		1.31	2.77	71	1.5	1.5	1.6	0.59	0.54	1.5

[a] Detected by rapid cooling. [b] A possibility of having a metastable phase. In ref 56, Henderson et al. have shown that [bmpro][(CF₃SO₂)₂N] has only a single melting peak at −3 °C, when the ionic liquid is fully crystallized by slow cooling.

TABLE 2: Solvatochromic Polarity Parameters of Room-Temperature Ionic Liquids

entry	RTIL	$E_T(30)$/kcal mol⁻¹	π^*	α	λ_{Cu}/nm
1	[bmim][(CF₃SO₂)₂N]	51.6	0.964	0.625	544
2	[bmim][BF₄]	52.2	1.04	0.610	540
3	[bmim][CF₃CO₂]	50.9	0.989	0.561	638
4	[bmim][PF₆]	52.4	1.02	0.636	517
5	[bmim][CF₃SO₃]	51.7	1.01	0.597	579
6	[bmim][(C₂F₅SO₂)₂)]	52.2	0.948	0.675	539
7	[(n-C₄H₉)(CH₃)₃N][(CF₃SO₂)₂N]	49.3	0.970	0.471	546
8	[bpy][(CF₃SO₂)₂N]	49.9	1.01	0.483	548
9	[bmpro][(CF₃SO₂)₂N]	48.2	0.945	0.411	548
10	[mmim][(CF₃SO₂)₂N]	52.4	0.993	0.664	546
11	[emim][(CF₃SO₂)₂N]	52.2	0.970	0.659	547
12	[C₆mim][(CF₃SO₂)₂N]	51.5	0.958	0.623	547
13	[C₈mim][(CF₃SO₂)₂N]	51.1	0.958	0.597	549

The $E_T(30)$ parameter, based on the large negative solvatochromic shift of the $\pi-\pi^*$ absorption band of Reichardt betaine dye, is one of the most common scales of solvating ability for a wide range of liquids.[5] The shift in the absorption band of the dye is mainly ascribed to the interaction between the phenoxide oxygen and the electron-accepting ability of the solvent by electron-pair donor/acceptor interactions and H-bond interactions. It has been reported that ca. 68% of the shift in

the transition energy is based on such specific solvation effects.[7] The solvatochromic shift is also well-known to have a good correlation with the AN of solvents.[8b] The $E_T(30)$ values of the present ionic liquids lie in the range of short-chain primary and secondary alcohols. Variations in the $E_T(30)$ values may depend on the cationic backbone structures. In the case of the [(CF$_3$-SO$_2$)$_2$N]-based RTILs with different cationic backbone structures (entries 1 and 7–9), the $E_T(30)$ values decreased in the following order: [bmim] > [bpy] > [(n-C$_4$H$_9$)(CH$_3$)$_3$N] > [bmpro]. However, the values of the [bmim]-based RTILs also show clear anionic effects, and increases in alkyl chain length in [Rmim]-[(CF$_3$SO$_2$)$_2$N] are also correlated with decreases in $E_T(30)$, as has been reported by several research groups.[36–38,47]

The linear solvation energy relationship, developed by Kamlet and Taft, is well-known as a quantitative multiparameter treatment of solvent effects, which makes use of the α, β, and π^* parameters (β is not discussed in the present paper).[7] The dipolarity/polarizability scale, π^*, can be obtained from a change in the absorption maximum wavelength for DENA, induced by the local electric field generated by the solvent.[7] Although the π^* values of the [Rmim][(CF$_3$SO$_2$)$_2$N] ionic liquids decrease with increasing alkyl chain length, no remarkable ionic structural dependence could be obtained for the case of changing anionic and cationic backbone structures (Table 2). In the RTILs, electrostatic forces from the ions, as well as dipole interactions and the polarizability effects, may affect the π^* values; these factors appear to explain the consistently high values in the present and previous studies.[38] Since the $E_T(30)$ values were affected not only by the change in the cationic backbone structure but also by the change in the anionic structure, the contribution from α was separately estimated (Table 2). The changes in the α values and the $E_T(30)$ values are similar, indicating that the betaine dye mainly detects the HBD ability of the RTILs. For the [bmim]-based RTILs with different anions (Table 2, entries 1–6), the α values should correlate with the HBA ability of the anions. The experimental order of the α values follows the order [bmim][(C$_2$F$_5$SO$_2$)$_2$N] > [bmim][PF$_6$] > [bmim][(CF$_3$SO$_2$)$_2$N] > [bmim][BF$_4$] > [bmim][CF$_3$SO$_3$] > [bmim][CF$_3$CO$_2$], indicating that the HBA abilities of the anions are not controlled only by their donor ability (vide supra). The existence of hydrophobic perfluorinated alkyl groups in the imide anions also contributes to the decreasing HBD ability.

Discussion

Anionic Structural Effects on $\Lambda_{imp}/\Lambda_{NMR}$. The ionic nature of the RTILs should be controlled by the types, magnitudes, and balances of the intermolecular forces, which are derived from the variations of the cationic and anionic structures. Figure 1a shows the relationship between λ_{Cu} and $\Lambda_{imp}/\Lambda_{NMR}$ for the [bmim]-based RTILs with different anionic structures (entries 1–6). The changes in λ_{Cu} correlate well with changes in $\Lambda_{imp}/\Lambda_{NMR}$, which clearly demonstrates that the formation of cation–anion aggregates in this group of RTILs is dominated by the anionic basicity. We have already reported the ab initio molecular orbital calculation of nine ion pairs of RTILs by changing the cationic and anionic structures.[48] In the calculated atomic charge distributions, the relatively high anionic donor abilities of [CF$_3$CO$_2$] and [CF$_3$SO$_3$] come from large negative charges on the oxygen atoms and their asymmetric distribution, which provide sites that can interact with the [bmim] cation. For the moderately donating [(CF$_3$SO$_2$)$_2$N], on the other hand, the negative charges are symmetrically distributed on nitrogen and four oxygen atoms. The low anionic donicities of [BF$_4$] and [PF$_6$] can be attributed to the equally distributed
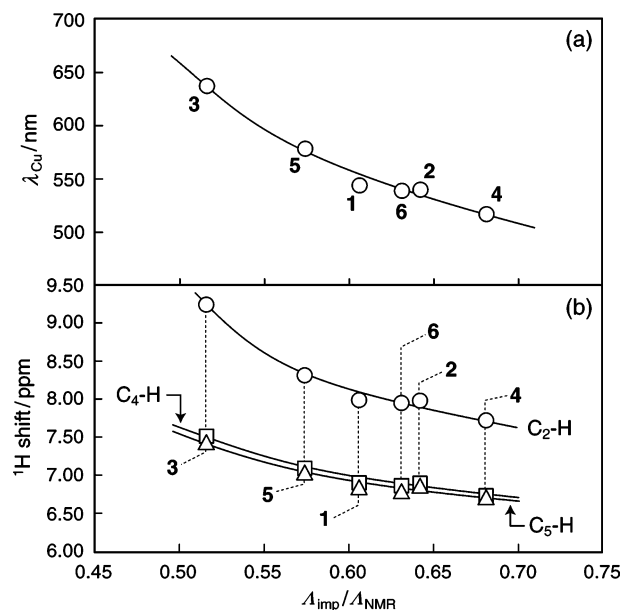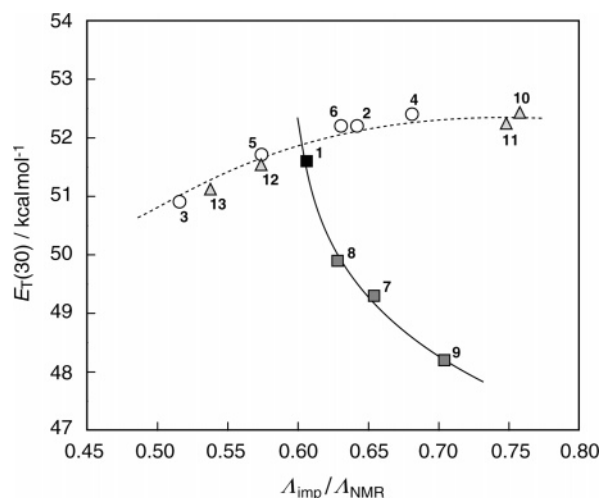

Figure 1. Relationship between $\Lambda_{imp}/\Lambda_{NMR}$ and (a) λ_{Cu} for [Cu(acac)-(tmen)]BPh$_4$ and (b) ^{1}H NMR chemical shifts for C$_2$-H (circles), C$_4$-H (squares), and C$_5$-H (triangles) on the imidazolium ring relative to external TMS in acetone-d_6 for [bmim]-based RTILs with different anionic structures: 1, [(CF$_3$SO$_2$)$_2$N]; 2, [BF$_4$]; 3, [CF$_3$CO$_2$]; 4, [PF$_6$]; 5, [CF$_3$SO$_3$]; and 6, [(C$_2$F$_5$SO$_2$)$_2$N]. The solid lines in the plots are guides for the eyes.

negative charge on the fluorine atoms and to the small absolute values. The calculated interaction energies (E_{int}) of the [emim]-based ion pairs were -89.8, -85.2, -82.6, -78.8, and -78.4 kcal mol^{-1} for [CF$_3$CO$_2$], [BF$_4$], [CF$_3$SO$_3$], [(CF$_3$SO$_2$)$_2$N], and [PF$_6$], respectively. The order of the absolute E_{int} values for the three organic anions ([CF$_3$CO$_2$] > [CF$_3$SO$_3$] > [(CF$_3$-SO$_2$)$_2$N]) and for the spherical inorganic anions ([BF$_4$] >[PF$_6$]) coincide well with the decreasing order of the anionic donicity, estimated by λ_{Cu}, and the increasing order of the $\Lambda_{imp}/\Lambda_{NMR}$ values. The spherical anions, with the equally distributed negative charge on the fluorine atoms, cause the loss of the specific interacting sites with the cation, which would be a reason for the lower $\Lambda_{imp}/\Lambda_{NMR}$ values compared to those of the organic anions.

Such an experimental relationship between the anionic structures and the $\Lambda_{imp}/\Lambda_{NMR}$ values was also confirmed by the ^{1}H NMR chemical shifts, measured by use of a double tube with neat RTIL in the inner tube and acetone-d_6 containing tetramethylsilane (TMS) in the outer tube. As can be seen in Figure 1b, the chemical shifts of the protons on the 2-, 4-, and 5-positions (C$_2$-H, C$_4$-H, and C$_5$-H, respectively) of the imidazolium ring increase with decreasing $\Lambda_{imp}/\Lambda_{NMR}$. The decrease in $\Lambda_{imp}/\Lambda_{NMR}$, i.e., increasing ionic association, leads to a decrease in the electron density of the protons on the imidazolium ring. The fact that the chemical shift for C$_2$-H is larger than those for C$_4$-H and C$_5$-H implies that the anions are likely to be situated close to the C$_2$-H on [bmim].

Cationic Structural Effects on $\Lambda_{imp}/\Lambda_{NMR}$. Figure 2 illustrates the relationship between $E_T(30)$ and $\Lambda_{imp}/\Lambda_{NMR}$ for the [(CF$_3$SO$_2$)$_2$N]-based RTILs having the same substituent butyl group with different cationic backbone structures (entries 1 and 7–9). With increasing $\Lambda_{imp}/\Lambda_{NMR}$ values, the $E_T(30)$ values decrease, indicating that Reichardt betaine dye reflects well the differences in the interactions between the [(CF$_3$SO$_2$)$_2$N] and these cations, specifically in this case the variation of cationic acceptor abilities.

Figure 2. Relationship between $\Lambda_{imp}/\Lambda_{NMR}$ and $E_T(30)$ for [bmim]-based RTILs with different anionic structures (circles) {1, [bmim][(CF$_3$SO$_2$)$_2$N]; 2, [bmim][BF$_4$]; 3, [bmim][CF$_3$CO$_2$]; 4, [bmim][PF$_6$]; 5, [bmim][CF$_3$SO$_3$]; and 6, [bmim][(C$_2$F$_5$SO$_2$)$_2$N]}, various [(CF$_3$SO$_2$)$_2$N]-based RTILs with different cationic backbone structures (squares) {7, [(n-C$_4$H$_9$)(CH$_3$)$_3$N][(CF$_3$SO$_2$)$_2$N]; 8, [bpy][(CF$_3$SO$_2$)$_2$N]; and 9, [bmpro]-[(CF$_3$SO$_2$)$_2$N]}, and various [Rmim][(CF$_3$SO$_2$)$_2$N] RTILs with different alkyl chain lengths {10, [mmim][(CF$_3$SO$_2$)$_2$N]; 11, [emim][(CF$_3$-SO$_2$)$_2$N]; 12, [C$_6$mim][(CF$_3$SO$_2$)$_2$N]; and 13, [C$_8$mim][(CF$_3$SO$_2$)$_2$N]}. The dashed and solid lines in the plot are guides for the eyes.

As reported previously,[48] the calculated E_{int} values for [BF$_4$] with [emim], 1-ethylpyridinium ([epy]), *N*-ethyl-*N*-methylpyrrolidinium ([empro]), and *N*-ethyl-*N*,*N*,*N*-trimethylammonium ([(C$_2$H$_5$)(CH$_3$)$_3$N]) were similar (−85.2, −82.8, −84.4, and −84.6 kcal mol^{-1}, respectively). However, the magnitudes of directional dependence of the interaction energy (E_{diff}), defined as the difference in the E_{int} values between the most stable and the least stable geometries, follows the order [emim] > [epy] ≈ [(C$_2$H$_5$)(CH$_3$)$_3$N] > [empro]. The positive charge of [emim] is located mainly on the C$_2$-H side of the imidazolium ring, which enables the anion to have close contact with the C$_2$-H. In contrast, the positive charges of the aliphatic [empro] and [(C$_2$H$_5$)(CH$_3$)$_3$N] are rather well distributed over the whole structures. In particular, the [empro] ion pair shows large numbers of isoenergetic local minima, relative to the other cations. In addition to the positive charge distribution, the round shape and steric hindrance would also prohibit the existence of clear interacting sites with the anion.

It is interesting to note that the order of the $\Lambda_{imp}/\Lambda_{NMR}$ values, i.e., the reverse order of the $E_T(30)$ values (Figure 2, entries 1 and 7−9), coincides with the reverse order of the E_{diff} values[48] for the RTILs having the same cationic backbone structures. This agreement implies that not only the magnitude of the interaction energy but also the magnitude of the directional dependency plays a crucial role in determining the formation of ionic aggregates of the RTILs. The relatively localized distribution of cationic charge for [bmim] and [bpy], as well as the aromatic plane structures, appears to enable the realization of close contacts with the anion, which also allows an interaction with the phenoxide of the betaine dye, leading to large $E_T(30)$ values. Such large directional dependence of the interaction would be a reason for the highest $E_T(30)$ and the lowest $\Lambda_{imp}/\Lambda_{NMR}$ of the [bmim] among the cations used in this study. It is well-known that the values of $E_T(30)$ and α decrease by substituting the C$_2$-H, having high acidity, on the imidazolium with a methyl group.[36,38] On the contrary, the small directional dependency would contribute to the largest $\Lambda_{imp}/\Lambda_{NMR}$ value of [bmpro] among the present RTILs.

Correlation between $E_T(30)$ and $\Lambda_{imp}/\Lambda_{NMR}$ under Chemical Equilibria. If the coordination ability of the imidazolium backbone to the betaine dye is the same in each RTIL, the estimated $E_T(30)$ values of the [bmim]-based RTILs with the different anions and the [Rmim][(CF$_3$SO$_2$)$_2$N] should be constant. However, focusing on the [bmim]-based RTILs (entries 1−6) and on the [Rmim][(CF$_3$SO$_2$)$_2$N] (entries 1 and 10−13) in Figure 2, $\Lambda_{imp}/\Lambda_{NMR}$ decreases with increasing anionic basicity and increasing alkyl chain length, which leads to a decrease in the $E_T(30)$ values (dashed line). The $\Lambda_{imp}/\Lambda_{NMR}-E_T(30)$ profile is opposite that for the [(CF$_3$SO$_2$)$_2$N]-based ionic liquids with different cationic backbone structures (solid line). This may be explained by a competition of two equilibria, one between the anion and the cations and a second between the probe dye and the cations, as has been suggested by Welton and co-workers.[38] Since the concentrations of the free cations depend on the extent of cation−anion aggregation, the decrease in the $\Lambda_{imp}/\Lambda_{NMR}$ values induces a decrease in the concentration of the free cations. This inhibits the formation of cation−betaine dye complex and thereby causes the $E_T(30)$ and α values to decrease (Table 2). The two opposite behaviors of the $\Lambda_{imp}/\Lambda_{NMR}-E_T(30)$ profiles clearly suggest that $E_T(30)$ depends not only on the cation−dye probe molecule interaction, but also on the degree of the formation of ionic aggregates. For the [bmim]-based RTILs, the formation of the cation−anion aggregates is dominated by the anionic donor abilities, whereas for the [Rmim][(CF$_3$SO$_2$)$_2$N] series, $\Lambda_{imp}/\Lambda_{NMR}$ decreases with increasing number of carbon atoms in the alkyl chain (see Table 1), as reported previously.[31b] The addition of a −CH$_2$− unit to the cation causes a decrease in the molar concentration, which relaxes the electrostatic attraction between the cation and the anion. On the other hand, the increase in the hydrocarbon chain length enhances the alkyl chain−ion inductive forces (dielectric polarization) and the hydrocarbon−hydrocarbon dispersive forces (van der Waals interaction). The decrease in the $\Lambda_{imp}/\Lambda_{NMR}$ values with increasing alkyl chain length indicates a significant contribution from the latter forces, compared to the electrostatic attractions.

Thus, the $\Lambda_{imp}/\Lambda_{NMR}$ values exhibit an excellent correlation with coordinating abilities of the cations and the anions and/or the overall interactions in the RTILs under chemical equilibria. Furthermore, these excellent correlations of the polarity scales and the NMR chemical shift with the $\Lambda_{imp}/\Lambda_{NMR}$ values suggest the possibility of using calibration curves for the estimation of the formation of ionic aggregates in the ionic liquids. For example, the $\Lambda_{imp}/\Lambda_{NMR}$ values estimated for [bmim][NO$_3$] and [bmim][CH$_3$CO$_2$] by use of reported values for $E_T(30)$ (51.8 for [bmim][NO$_3$] and 49.2 for [bmim][CH$_3$CO$_2$])[47] are 0.55 and <0.4, respectively, which can be easily imagined to be true on the basis of the acidities of the conjugate acids.

Ionic Concentration and Vapor Pressure. The RTILs having large amounts of ionic aggregates may have higher vapor pressures than ideally unassociated salts. Normal boiling temperatures (T_b), which correlate with the vapor pressure at 1 atm, cannot be experimentally determined for typical RTILs, because of decomposition prior to reaching T_b. However, Rebelo and co-workers have predicted the normal T_b values for [Rmim]-[X] ([X] = [BF$_4$], [PF$_6$], and [(CF$_3$SO$_2$)$_2$N]), by using the critical points (T_c's) estimated from the experimental surface tension and the density data, and the empirical rule that T_b is approximately $0.6T_c$ for most substances.[49] The predicted T_b values for the [Rmim][X]-based ionic liquids decrease with increasing alkyl chain length. For the case of varying anionic structures with a fixed alkyl chain length for [Rmim], T_b follows the order
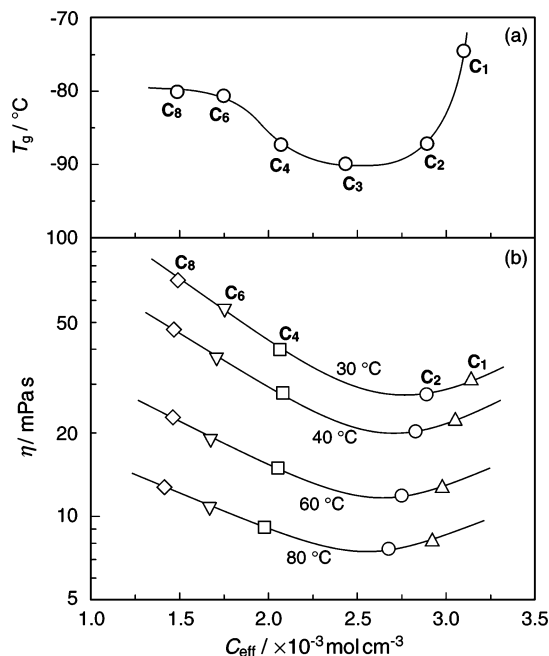
Figure 3. C_{eff} dependency of (a) T_g and (b) viscosity for [Rmim][(CF$_3$-SO$_2$)$_2$N] RTILs with different alkyl chain lengths. C_n in the plots indicates the number of carbon atoms in the alkyl chain of [Rmim]. The T_g value of C_1 is estimated by $T_g/T_m = 2/3$, i.e., "the two-thirds rule", and C_3 is cited by ref 17. The symbols in the bottom figure exhibit different alkyl chain lengths of [Rmim]: triangles, C_1; circles, C_2; squares, C_4; inverted triangles, C_6; and diamonds, C_8. The solid lines in the plots are guides for the eyes.

[BF$_4$] > [PF$_6$] > [(CF$_3$SO$_2$)$_2$N]. The C_{eff} value for [bmim]-based RTILs follows the order [BF$_4$] > [PF$_6$] > [(CF$_3$SO$_2$)$_2$N], and that for the [Rmim][(CF$_3$SO$_2$)$_2$N] series decreases with increasing alkyl chain length, which correlates well with the order of the estimated normal T_b values.

The reduction of the C_{eff}, thus, seems to correlate with the vapor pressure for the ionic liquids. Recently, Earle and co-workers have demonstrated that ionic liquids can be distilled at 200−300 °C under highly reduced pressure and then recondensed at low temperature.[50] They have reported that the vapor pressure for [CF$_3$SO$_3$]-based RTILs seems lower than for similar [(CF$_3$SO$_2$)$_2$N] ionic liquids, as shown by their low distillation rate (<0.01 g h^{-1}), and that the [PF$_6$] ionic liquids distilled very slowly with little decomposition. It is worth mentioning here that we have reported[51] the transport properties of a molten lithium salt, LiAl[OCH(CF$_3$)$_2$]$_4$, having the low melting point of 119 °C. The properties in the molten state at 130 °C are characterized by the high self-diffusion coefficients of ^{7}Li and ^{1}H (4.8 × 10^{-6} and 4.3 × 10^{-6} cm^2 s^{-1}, respectively) and the poor ionic conductivity (1.4 × 10^{-5} S cm^{-1}).[51] The poor conductivity with the high diffusivity could be ascribed to the low $\Lambda_{imp}/\Lambda_{NMR}$ value of 1.9 × 10^{-4}, which results in the quite low C_{eff} of 5.3 × 10^{-7} mol cm^{-3}. The sublimation of LiAl-[OCH(CF$_3$)$_2$]$_4$ under reduced pressure would be attributed to its negligible ionic concentration.

Liquid-State Dynamics of RTILs. Relatively weak inductive and dispersive forces, compared with electrostatic attractions, can play important roles in determining the liquid-state dynamics. Figure 3 illustrates the C_{eff} dependence of (a) the glass transition temperature T_g and (b) the isothermal viscosities for the [Rmim][(CF$_3$SO$_2$)$_2$N] series with different alkyl chain lengths. T_g is well-known as one of the most important physical parameters controlling the fluidity of amorphous materials. Since glasses are disordered materials, which lack the periodicity of

crystals, the glass formation can be explained by energetic considerations, different from crystallization, which includes an entropy term in the transition. Therefore, the minimum in the $T_g−C_{eff}$ profile can be explained by a competition between the electrostatic forces and the inductive and dispersive forces. A decrease in the C_{eff} contributes to relaxing the electrostatic forces among oppositely charged ions, which should result in decreasing T_g (electrostatic forces controlled region, $C_1−C_3$ in Figure 3a). On the other hand, such a decrease in C_{eff}, due to an increase in the alkyl chain length in this case, also causes an increase in the inductive and dispersive forces, which leads to an enhancement of T_g, owing to frictional forces among the ion aggregates and clusters (inductive and dispersive forces controlled region, $C_3−C_8$ in Figure 3a).[52] The viscosity of ionic liquids seems to be determined by many parameters, such as molecular weight, shape and size of the ions, and intermolecular and interionic interactive forces. However, the minima of viscosity−C_{eff} profiles (Figure 3b) strongly indicate that the viscosity can also be explained by a competition between the interactive forces. The minima of viscosity as a function of the number of carbon atoms in the alkyl chain have also been reported in some combinations of cationic and anionic structures, such as [Rmim]-based RTILs with [Al$_2$Cl$_7$][53] and [CF$_3$BF$_3$],[15b] and 1-alkylpyridinium-based liquids with [Al$_2$Cl$_7$].[54] Since the reduction of the ionic concentration with increasing alkyl chain length appears to be a common feature in the examples, these RTILs would also exhibit the minima as a function of the C_{eff}. The higher viscosity of [bmim][(C$_2$F$_5$SO$_2$)$_2$N] than that of [bmim]-[(CF$_3$SO$_2$)$_2$N] (Table 1, entries 1 and 6) would also be interpreted by a significant contribution from the inductive and dispersive forces derived from longer perfluoroalkyl chain length, rather than relaxation of the electrostatic forces.

Although the simple competition between the electrostatic forces and the inductive and dispersive forces in the [Rmim]-[(CF$_3$SO$_2$)$_2$N] series provides a characteristic aspect of the liquid-state dynamics, the variation of the anions and the cationic backbones causes a drastic change in the magnitudes and balances of these interactions. The C_{eff} value focuses only on the electrostatic forces based on the average effective ionic distance, which results in a limitation for a systematic illustration for the ionic structural effects on the physical properties (T_g and viscosity) for the other RTILs in this study. For instance, the [(CF$_3$SO$_2$)$_2$N]-based RTILs with different cationic backbone structures have almost the same C_{eff} values (Table 1, entries 1 and 7−9), implying that the different physical properties are caused by differences in the inductive and dispersive forces, rather than electrostatic attraction. Although the lower viscosity of [bmim][BF$_4$] compared to that of [bmim][PF$_6$] cannot be explained, the C_{eff} dependence of viscosities for [bmim]-based RTILs with different anions (Table 1, entries 1−5, except for [bmim][(C$_2$F$_5$SO$_2$)$_2$N]), as is depicted in Figure 4, suggests that the viscosity of the other [bmim] series would be mainly dominated by electrostatic attractions. Therefore, the estimation of C_{eff}, by use of the $\Lambda_{imp}/\Lambda_{NMR}$−polarity scale (vide supra), can be a useful guideline for the prediction of the physical properties for certain RTILs. For example, by use of the reported density data at 30 °C (1.1497 g cm^{-3}) for [bmim][NO$_3$][55] and an estimated $\Lambda_{imp}/\Lambda_{NMR}$ value of 0.55, C_{eff} is calculated to be 3.1 × 10^{-3} mol cm^{-3}. A plot of [bmim][NO$_3$] in Figure 4 using the calculated C_{eff} and the reported viscosity value (144 mPa s)[55] at that temperature agrees well with the expected C_{eff}−viscosity profile (solid line in Figure 4).

Physicochemical Properties of RTILs

J. Phys. Chem. B, Vol. 110, No. 39, 2006 **19599**
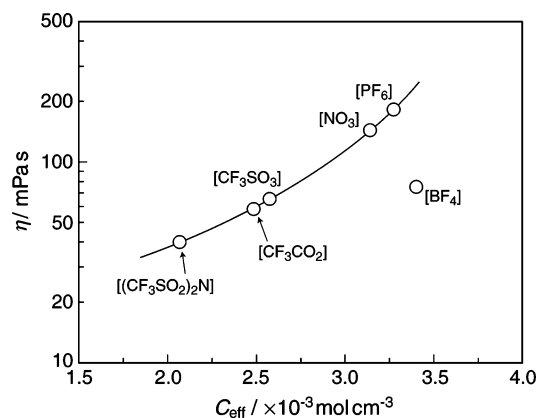
Figure 4. C_{eff} dependency of viscosity for [bmim][(CF$_3$SO$_2$)$_2$N] RTILs with different anionic structures. For [bmim][NO$_3$], the viscosity data are from the literature;[55] the C_{eff} was calculated from the density value[55] and $\Lambda_{imp}/\Lambda_{NMR}$ was estimated from reported $E_T(30)$ value[47] and Figure 2. The solid lines in the plots are guides for the eyes.

Conclusion

The ionic nature of the RTILs, defined as $\Lambda_{imp}/\Lambda_{NMR}$ in this study, is controlled by the magnitudes and balances of the interactive forces, which can be explained by the effects of anionic donor and cationic acceptor abilities for RTILs having either different types of anions with the same cation, or vice versa, and by the inductive and dispersive forces for the [Rmim]-based RTILs with the various alkyl chain lengths. Although some of the solvatochromic polarity scales do not illustrate well the ionic state of the RTILs, $\Lambda_{imp}/\Lambda_{NMR}$ does illustrate the degree of cation−anion aggregation in all of the ionic liquids at chemical equilibrium. It may be possible to estimate the $\Lambda_{imp}/\Lambda_{NMR}$ values for common RTILs by use of the $\Lambda_{imp}/\Lambda_{NMR}$−polarity profile and/or the ^{1}H NMR chemical shift profile as calibration curves. A decrease in C_{eff}, representing the effective electrostatic forces in the RTILs, may induce an increase in vapor pressure, whereas the liquid-state dynamics, such as T_g and viscosity, are controlled by a subtle balance between the electrostatic and other intermolecular forces. The C_{eff} value could be one of the more useful parameters for the estimation of the physical properties of the RTILs.

Experimental Section

The syntheses of all of the RTILs in this study were based on a metathesis reaction of freshly prepared halide salts of the imidazolium cation and alkali metal salts with different anions, as described our in previous reports,[31] and stored in an argon atmosphere glovebox (VAC, [O$_2$] < 1 ppm, [H$_2$O] < 1 ppm). The experimental values of the thermal properties, density, ionic self-diffusion coefficients, viscosity, and ionic conductivity presented in this paper are taken from the original data found in our earlier reports.[31] The solvatochromic dyes, Reichardt's betaine dye (Aldrich) and DENA (Fluka), were used as received, and [Cu(acac)(tmen)]BPh$_4$ was synthesized following a reported procedure.[45] All of the sample preparation for solvatochromic UV−visible and ^{1}H NMR measurements was conducted in the glovebox. For the solvatochromic measurements, the mixtures of the RTILs and the probe dye solutes were placed in a quartz cell (M25-UV-2, GL Science Inc.) and were tightly sealed. All the absorbance measurements were carried out by use of a computer-controlled Shimazu UV-2500PC, equipped with a thermoregulated water bath (NCB-3100, Tokyo Rikakikai Co. Ltd.). The $E_T(30)$, π^*, and α values were calculated by use of the following equations:

$$E_T(30) = 28591/\lambda_{betaine} \tag{2}$$

$$\pi^* = 0.314(27.52 - 10^4/\lambda_{DENA}) \tag{3}$$

$$\alpha = 0.0649[E_T(30)] - 2.03 - 0.72\pi^* \tag{4}$$

where $\lambda_{betaine}$ and λ_{DENA} (in nm) are the maximum absorbance wavelengths of Reichardt's betaine dye and the DENA, respectively. For the ^{1}H NMR measurements, the Fourier transform NMR spectra were obtained on a JEOL JNM-AL 400 spectrometer. The ^{1}H NMR chemical shifts were determined by use of a double tube (SC-008, Shigemi Co. Ltd.; inner tube, 2.5 mm i.d., 3.29 mm o.d.; outer tube, 4.2 mm i.d., 4.965 mm o.d.; spacer, 3.3 mm i.d., 4.19 mm o.d.) with the sample in the inner tube and acetone-d_6 containing TMS as standard in the outer tube.

Supporting Information Available: Experimental data of densities, self-diffusion coefficients for cations and anions, viscosities, and ionic conductivities for RTILs used in the present study for the entire measured temperature range. This material is available free of charge via the Internet at http://pubs.acs.org.

References and Notes

(1) *Ionic Liquids in Synthesis*; Wasserscheid, P., Welton, T., Eds.; Wiley-VCH: Weinheim, Germany, 2003.

(2) (a) Welton, T. *Chem. Rev.* **1999**, *99*, 2071−2083. (b) Holbrey, J. D.; Seddon, K. R. *Clean Prod. Process.* **1999**, *1*, 223−236. (c) Wassersheid, P.; Keim, W. *Angew. Chem., Int. Ed.* **2000**, *39*, 3772−3789. (d) Wilkes, J. S. *J. Mol. Catal. A: Chem.* **2004**, *214*, 11−17.

(3) (a) Kosower, E. M. *J. Am. Chem. Soc.* **1958**, *80*, 3253−3260. (b) Kosower, E. M.; Skorcz, J. A.; Schwarz, W. M.; Patton, J. W. *J. Am. Chem. Soc.* **1960**, *82*, 2188−2191.

(4) Grunwald, E.; Winstein, S. *J. Am. Chem. Soc.* **1948**, *70*, 846−854.

(5) (a) Reichardt, C. *Chem. Rev.* **1994**, *94*, 2319−2358. (b) *Solvent and Solvent Effects in Organic Chemistry*; Reichardt, C., Ed.; Wiley-VCH: New York, 2003.

(6) (a) Dong, D. C.; Winnik, M. A. *Photochem. Photobiol.* **1982**, *35*, 17−21. (b) Dong, D. C.; Winnik, M. A. *Can. J. Chem.* **1984**, *62*, 2560−2565.

(7) (a) Kamlet, M. J.; Taft, R. W. *J. Am. Chem. Soc.* **1976**, *98*, 377−383. (b) Taft, R. W.; Kamlet, M. J. *J. Am. Chem. Soc.* **1976**, *98*, 2886−2894. (c) Kamlet, M. J.; Abboud, J. L.; Taft, R. W. *J. Am. Chem. Soc.* **1977**, *99*, 6027−6038. (d) Kamlet, M. J.; Abboud, J. L.; Abraham, M. H.; Taft, R. W. *J. Org. Chem.* **1983**, *48*, 2877−2887.

(8) (a) Gutmann, V. *Coord. Chem. Rev.* **1976**, *18*, 225−255. (b) Gutmann, V. *The Donor-Acceptor Approach to Molecular Interaction*; Plenum: New York, 1978.

(9) Bonhôte, P.; Dias, A.-P.; Papageorgiou, N. Kalyanasundaram, K.; Grätzel, M. *Inorg. Chem.* **1996**, *35*, 1168−1178.

(10) (a) Holbrey, J. D.; Seddon, K. R. *Clean Prod. Process.* **1999**, *1*, 223−236. (b) Holbrey, J. D.; Seddon, K. R. *J. Chem. Soc., Dalton Trans.* **1999**, 2133−2139.

(11) (a) Sun, J.; MacFarlane, D. R.; Forsyth, M. *Ionics* **1997**, *3*, 356−362. (b) Sun, J.; Forsyth, M.; MacFarlane, D. R. *J. Phys. Chem. B* **1998**, *102*, 8858−8864. (c) MacFarlane, D. R.; Meakin, P.; Sun, J.; Amini, N.; Forsyth, M. *J. Phys. Chem. B* **1999**, *103*, 4164−4170.

(12) (a) MacFarlane, D. R.; Forsyth, S. A.; Golding, J.; Deacon, G. B. *Green Chem.* **2002**, *4*, 444−448. (b) Pringle, J. M.; Golding, J.; Forsyth, C. M.; Deacon, G. B.; Forsyth, M.; MacFarlane, D. R. *J. Mater. Chem.* **2002**, *12*, 3457−3480.

(13) Forsyth, S. A.; MacFarlane, D. R. *J. Mater. Chem.* **2003**, *13*, 2451−2456.

(14) (a) Matsumoto, H.; Yanagida, M.; Tanimoto, K.; Nomura, M.; Kitagawa, Y.; Miyazaki, Y. *Chem. Lett.* **2000**, 922−923. (b) Matsumoto, H.; Matsuda, T.; Miyazaki, Y. *Chem. Lett.* **2000**, 1430−1431. (c) Matsumoto, H.; Kageyama, H.; Miyazaki, Y. *Chem. Lett.* **2001**, 182−183.

(15) (a) Zhou, Z.-B.; Takeda, M.; Ue, M. *J. Fluorine Chem.* **2004**, *125*, 471−476. (b) Zhou, Z.-B.; Matsumoto, M.; Tatsumi, K. *Chem. Lett.* **2004**, 680−681. (c) Zhou, Z.-B.; Matsumoto, M.; Tatsumi, K. *Chem. Lett.* **2004**, 886−887.

(16) (a) Koch, V. R.; Dominey, L. A.; Nanjundiah, C.; Ondrechen, J. *J. Electrochem. Soc.* **1996**, *143*, 798−803. (b) Nanjundiah, C.; McDevitt, S. F.; Koch, V. R. *J. Electrochem. Soc.* **1997**, *144*, 3392−3397. (c) MacEwen, A. B.; Ngo, H. L.; LeCompte, K.; Goldman, J. L. *J. Electrochem. Soc.* **1999**, *146*, 1687−1695.

(17) Ngo, H. L.; LeCompte, K.; Hargen, L.; McEwen, A. B. *Thermochim. Acta* **2000**, *357−358*, 97−102.

(18) (a) Fox, D. M.; Awad, W. H.; Gilman, J. W.; Maupin, P. H.; DeLong, H. C.; Trulove, P. C. *Green Chem.* **2003**, *5*, 724−727. (b) Awad, W. H.; Gilman, J. W.; Nyden, M.; Harris, R. H.; Sutto, T. E.; Callahan, J.; Trulove, P. C.; DeLong, H. C.; Fox, D. M. *Thermochim. Acta* **2004**, *409*, 3−11.

(19) Huddleston, J. G.; Visser, A. E.; Reichart, W. M.; Willauer, H. D.; Broker, G. A.; Rogers, R. D. *Green Chem.* **2001**, *3*, 156−164.

(20) Hagiwara, R.; Matsumoto, K.; Nakamori, Y.; Tsuda, T.; Ito, Y.; Matsumoto, H.; Momota, K. *J. Electrochem. Soc.* **2003**, *150*, D195−D199.

(21) (a) Cammarata, L.; Kazarian, S. G.; Salter, P. A.; Welton, T. *Phys. Chem. Chem. Phys.* **2001**, *3*, 5192−5200. (b) Seddon, K. R.; Stark, A.; Torres, M. J. *Pure Appl. Chem.* **2000**, *72*, 2275−2287.

(22) (a) Armstrong, D. W.; He, L.; Liu, Y.-S. *Anal. Chem.* **1999**, *71*, 3873−3876. (b) Anthony, J. L.; Maginn, E. J.; Brennecke, J. F. *J. Phys. Chem. B* **2001**, *105*, 10942−10949. (c) Blanchard, L. A.; Gu, Z.; Brennecke, J. F. *J. Phys. Chem. B* **2001**, *105*, 2437−2444.

(23) Lancaster, N. L.; Salter, P. A.; Welton, T.; Young, G. B. *J. Org. Chem.* **2002**, *67*, 8855−8861.

(24) Meng, Z.; Dolle, A.; Carper, W. R. *J. Mol. Struct. (THEOCHEM)* **2002**, *585*, 119−128.

(25) Turner, E. A.; Pye, C. C.; Singer, R. D. *J. Phys. Chem. A* **2003**, *107*, 2277−2288.

(26) Liu, Z.; Huang, S.; Wang, W. *J. Phys. Chem. B* **2004**, *108*, 12978−12989.

(27) Morrow, T. I.; Magninn, E. J. *J. Phys. Chem. B* **2002**, *106*, 12807−12813.

(28) (a) Hanke, C. G.; Atmas, N. A.; Lynden-Bell, R. M. *Green Chem.* **2002**, *4*, 107−111. (b) Hanke, C. G.; Lynden-Bell, R. M. *J. Phys. Chem. B* **2003**, *107*, 10873−10878. (c) Hanke, C. G.; Johansson, A.; Harper, J. B.; Lynden-Bell, R. M. *Chem. Phys. Lett.* **2003**, *374*, 85−90.

(29) (a) Chaumont, A.; Engler, E.; Wipff, G. *Inorg. Chem.* **2003**, *42*, 5348−5356. (b) Chaumont, A.; Wipff, G. *Phys. Chem. Chem. Phys.* **2003**, *5*, 3481−3488. (c) Chaumont, A.; Wipff, G. *J. Phys. Chem. B* **2004**, *108*, 3311−3319.

(30) Noda, A.; Hayamizu, K.; Watanabe, M. *J. Phys. Chem. B* **2001**, *105*, 4603−4610.

(31) (a) Tokuda, H.; Hayamizu, K.; Ishii, K.; Susan, M. A. B. H.; Watanabe, M. *J. Phys. Chem. B* **2004**, *108*, 16593−16600. (b) Tokuda, H.; Hayamizu, K.; Ishii, K.; Susan, M. A. B. H.; Watanabe, M. *J. Phys. Chem. B* **2005**, *109*, 6103−6110. (c) Tokuda, H.; Ishii, K.; Susan, M. A. B. H.; Tsuzuki, S.; Hayamizu, K.; Watanabe, M. *J. Phys. Chem. B* **2006**, *110*, 2833−2839.

(32) (a) Fitzgerald, J. V. *J. Chem. Phys.* **1952**, *20*, 922. (b) Haven, Y.; Verkerk, B. *Phys. Chem. Glasses* **1965**, *6*, 38−45.

(33) (a) Hayamizu, K.; Aihara, Y.; Arai, S.; Martinez, C. G. *J. Phys. Chem. B* **1999**, *103*, 519−524. (b) Aihara, Y.; Sugimoto, K.; Price, W. S.; Hayamizu, K. *J. Chem. Phys.* **2000**, *113*, 1981−1991. (c) Aihara, Y.; Bando, T.; Nakagawa, H.; Yoshida, H.; Hayamizu, K.; Akiba, E.; Price, W. S. *J. Electrochem. Soc.* **2004**, *151*, A199−A122.

(34) Carmichael, A. J.; Seddon, K. R. *J. Phys. Org. Chem.* **2000**, *13*, 591−595.

(35) Aki, S. N. V. K.; Brennecke, J. F.; Samanta, A. *Chem. Commun.* **2001**, 413−414.

(36) Muldoon, M. J.; Gordon, C. M.; Dunkin, I. R. *J. Chem. Soc., Perkin Trans. 2* **2001**, 433−435.

(37) Dzyuba, S. V.; Bartsch, R. A. *Tetrahedron Lett.* **2002**, *43*, 4657−4659.

(38) Crowhurst, L.; Mawdsley, P. R.; Arlandis, J. M. P.; Salter, P. A.; Welton, T. *Phys. Chem. Chem. Phys.* **2003**, *5*, 2790−2794.

(39) Fletcher, K. A.; Pandey, S. *J. Phys. Chem. B* **2003**, *107*, 13532−13539.

(40) Baker, S. N.; Baker, G. A.; Kane, M. A.; Bright, F. V. *J. Phys. Chem. B* **2001**, *105*, 9663−9668.

(41) (a) Karmakar, R.; Samanta, A. *J. Phys. Chem. A* **2002**, *106*, 4447−4452. (b) Karmakar, R.; Samanta, A. *J. Phys. Chem. A* **2002**, *106*, 6670−6675.

(42) Ingram, J. A.; Moog, R. S.; Ito, N.; Biswas, R.; Maroncelli, M. *J. Phys. Chem. B* **2003**, *107*, 5926−5932.

(43) Baker, S. N.; Baker, G. A.; Munson, C. A.; Chen, F.; Bukowski, E. J.; Cartwright, A. N.; Bright, F. V. *Ind. Eng. Chem. Res.* **2003**, *42*, 6457−6463.

(44) Hyun, B.-R.; Dzyuba, S. V.; Bartsch, R. A.; Quitevis, E. L. *J. Phys. Chem. A* **2002**, *106*, 7579−7585.

(45) (a) Fukuda, Y.; Sone, K. *Bull. Chem. Soc. Jpn.* **1972**, *45*, 465−469. (b) Soukup, R. W.; Sone, K. *Bull. Chem. Soc. Jpn.* **1987**, *60*, 2286−2288.

(46) Linert, W.; Jameson, R. F.; Taha, A. *J. Chem. Soc., Dalton Trans.* **1993**, 3181−3186.

(47) Karr, J. L.; Jesionowski, A. M.; Berberich, J. A.; Moulton, R.; Russel, A. J. *J. Am. Chem. Soc.* **2003**, *125*, 4125−4131.

(48) Tsuzuki, S.; Tokuda, H.; Hayamizu, K.; Watanabe, M. *J. Phys. Chem. B* **2005**, *109*, 16474−16481.

(49) Rebelo, L. P. N.; Lopes, J. N. C.; Esperança, J. M. S. S.; Filipe, E. *J. Phys. Chem. B* **2005**, *109*, 6040−6043.

(50) Earle, M. J.; Esperança, J. M. S. S.; Gilea, M. A.; Lopes, J. N. C.; Rebelo, L. P. N.; Magee, J. W.; Seddon, K. R.; Widegren, J. A. *Nature* **2006**, *439*, 831−834.

(51) Tokuda, H.; Tabata, S.; Susan, M. A. B. H.; Hayamizu, K.; Watanabe, M. *J. Phys. Chem. B* **2004**, *108*, 11995−12002.

(52) Strictly, the C_{eff} at T_g should be used for this figure. However, the extrapolated molar concentration for the [Rmim][(CF$_3$SO$_2$)$_2$N] series at T_g is larger only by ca. 8% compared with the values at 30 °C, and furthermore, the order of the molar concentration is the same at the measured temperature range, as well as the order of $\Lambda_{imp}/\Lambda_{NMR}$ values. Therefore, we have adopted the C_{eff} value at 30 °C as a typical example representing the order of the average ionic distance at T_g.

(53) Wilkes, J. S.; Levisky, J. A.; Wilson, R. A.; Hussey, C. L. *Inorg. Chem.* **1982**, *21*, 1263−1264.

(54) Carpio, R. A.; King, L. A.; Lindstrom, R. E.; Ward, E. H.; Hussey, C. L. *J. Electrochem. Soc.* **1979**, *126*, 1644−1649.

(55) Seddon, K. R.; Stark, A.; Torres, M.-J. Viscosity and density of 1-alkyl-3-methylimidazonium ionic liquids. In *Clean Solvents*; Abraham, M., Moens, L., Eds.; American Chemical Society: Washington, DC, 2002; Vol. 819, pp 34−49.

(56) Henderson, W. A.; Passerini, S. *Chem. Mater.* **2004**, *16*, 2881−2885.